CHINESE OPTICS LETTERS

Vol. 21, No. 10 | October 2023

Parallel all-optical logic operations based on metasurface polarization optics

Jing Wang (王 婧)[1], Wenli Wang (汪文莉)[2], Yang Lu (陆 洋)[1], Qun Hao (郝 群)[2], and Liandong Yu (于连栋)[1*]

[1] China University of Petroleum, Qingdao 266580, China

[2] Beijing Institute of Technology, Beijing 100081, China

*Corresponding author: liandongyu@upc.edu.cn

Received February 23, 2023 | Accepted May 31, 2023 | Posted Online October 10, 2023

We developed a general framework for parallel all-optical logic operations with independent phase control of arbitrary orthogonal polarization state enabled by a single-layer metasurface. A pair of orthogonal circular polarized bases are used as two input channels of the logic operator, and their four combinations perfectly match various binary input states. Correspondingly, distinct phase profiles are encoded into the metasurface, which enables parallel operation of the two logic gates by way of polarization switching. It allows for an efficient and compact way to implement multi-channel multiplexed logic gate operations with the capability of fast optical computing at the chip scale.

Keywords: parallel all-optical logic operation; metasurface; polarization.

DOI: 10.3788/COL202321.101602

1. Introduction

All-optical computing has aroused great concern for some time, as the current energy efficiency of digital electronics cannot meet the rapid growth of computing loads[1–3]. Light-based devices show powerful capabilities in fast signal processing over electronic counterparts since photonic circuits can eliminate the restriction of running speed and heat loss with photons instead of electrons[4,5]. As the fundamental building block of computing, optical logic operation holds large potential in the field of nano-photonics and integrated optics. Previously reported optical logic gates mainly use multi-beam interference or nonlinear effects, which have strict and complex operational requirements. Specifically, the phase difference needs to be precisely controlled for multi-beam interference so that the intensity contrast ratio between the output binary logic "1" and "0" can be effectively realized[6,7]. To ensure the generation of nonlinear effects, the use of high optical power is demanded, which is unfavorable in practical optical systems[8,9]. In addition, the introduction of bulky apparatus has greatly hindered the miniaturization and integration of the logic operators, which is not applicable to the implementation of an optical network at the chip scale. Thus, ultracompact metasurface-based operators are urgently needed for the advancement of optical logic gates, which provide a promising solution for simplifying the operation process and removing the bulky configurations.

Metasurface, two-dimensional versions of metamaterials, can manipulate the phase, amplitude, polarization, and orbital angular momentum of incident electromagnetic waves using subwavelength arrays of optical phase-shifting elements[10–12]. They have provided a scalable platform for various applications, such as metalens[13,14], LiDAR[15,16], and color display[17,18]. Especially, metasurface-based optical computing is booming and progressing due to its multifunctionality, miniaturization, and CMOS compatibility[19,20]. Recently, metasurface-based logic operators have been demonstrated by partially mimicking a trained diffractive neural network, which opens a new pathway toward photonic networks with miniaturization and integration. When input light strikes the specific regions of the metasurface (mode selection for logic gates), corresponding binary logic "1" or "0" can be presented in the form of a light spot on the output layer[21,22]. That means an optical mask for mode activation of the input layer is necessary in a neural network-based logic operator. This will inevitably create difficulties in calibration and installation, which is not conducive to the further development of integrated optical systems.

Here, we propose and demonstrate a single-layer metasurface-based logic operator that can perform two logic gates in parallel. A pair of orthogonal circular polarized bases are used as two input channels of the logic operator, and their four combinations perfectly match various binary input states. According to the generalized Snell's law of transmission, an abrupt phase can be encoded on a 2D planar metasurface, allowing for flexible wavefront engineering. By assigning multiple independent phase gradients to two orthogonal polarizations, off-axis bifocus and one focus can, respectively, be realized under the incidence of circularly polarized and linearly polarized light[23]. The results show that it perfectly matches the mechanism of Boolean

logic operations by reasonably designing the phase profile. Thus, the framework of a bi-logic operator can be built using a microchip vertical-cavity surface-emitting laser, which is attractive in all-optical logic operations with polarization-bistability[24–27]. The proposed multiplex bi-logic operator features no alignment problems and suffers from negligible crosstalk with a single noninterleaved metasurface. More importantly, wavefront engineering with the Jones matrix metasurface allows flexible expansion of a few logic operations channel capacity without degrading the quality of logic operations.

2. Principle and Design

Figure 1 schematically shows the parallel optical logic operator based on a polarization-switchable bi-focus metalens. As shown in Fig. 1(a), we adopt right-hand circularly polarized light (RCP, input channel 1) and left-hand circularly polarized light (LCP, input channel 2) as the two input channels. Then, polarization-tunable off-axis focusing can be achieved on the focusing plane according to distinct input conditions. Specifically, there are two off-axis focal spots under the incidence of RCP or LCP, while there is only one off-axis focal spot under the X linearly polarized light (XLP, a combination of RCP and LCP). In the parallel logical operations, a pair of orthogonal circularly polarized lights are employed as the two input channels, where binary input level ("1" or "0") is determined by the light intensity in the corresponding channel. Thus, the input signals with RCP, LCP, and XLP are denoted as (1, 0), (0, 1), and (1, 1), and no input is represented as (0, 0). The binary logic output ("1" or "0") directly depends on whether there is a spot in the design area of the focal plane. Here, off-axis focal spot 1 ($x = +3.5\,\mu$m) is designed as the "OR" gate, and off-axis focal spot 2 ($x = -3.5\,\mu$m) is designed as the "XOR" or the "NOT" logic gate.

Figure 1(b) displays the detailed logic operations under distinct input conditions. Focal spot 1 can be achieved as long as there is an input beam, which is the logic function of the "OR" gate. In other words, the inputs (1, 0), (0, 1), and (1, 1) correspond to binary logic output "1", while the input (0, 0) corresponds to binary logic output "0". Also, focal spot 2 can be realized only when one of the input channels is activated, which is the performance of the "XOR" gate. That is, binary logic output "1" can be achieved under the input (1, 0) or (0, 1), and binary logic output "0" is performed under the input (0, 0) or (1, 1). Moreover, focal spot 2 can also be used as the logic output of the "NOT" gate. Here, the RCP input channel serves as the control port, which can provide power to ensure the logic operation. The LCP input channel is used as the binary logic input of the "NOT" gate. Correspondingly, the incidence of the LCP leads to the logic output "0", and the incidence without the LCP leads to logic output "1".

We then progress to the design principle of the polarization-switchable bi-focus metalens, which can be used to implement a parallel optical logic operation. The wavefront modulation of metasurfaces is manipulated by the optical responses of its composed meta-atoms. Here, each meta-unit can be regarded as a linearly birefringent wave plate with the Jones matrix expressed as

$$J = R(-\theta)\begin{pmatrix} e^{i\phi_x} & 0 \\ 0 & e^{i\phi_y} \end{pmatrix} R(\theta), \tag{1}$$

where ϕ_x and ϕ_y separately represent the phase shifts acting along the fast axis and slow axis, which can be modified by

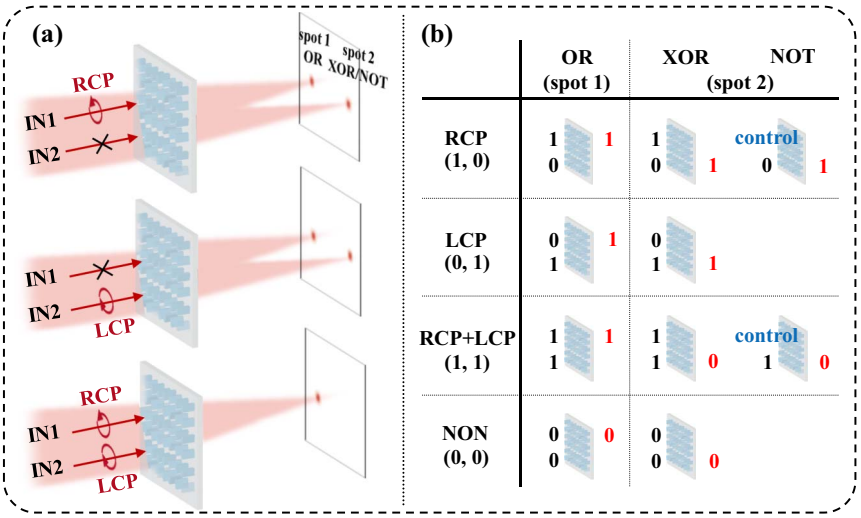

Fig. 1. Working principle of the parallel logic operation based on the metasurface polarization optics. (a) Polarization-tunable focusing effects of the noninterleaved metalens under diverse polarized light. RCP is adopted as the input channel 1 (IN1) and LCP is used as the input channel 2 (IN2). Focal spot 1 is designed for the "OR" logic gate, and focal spot 2 is used for the "XOR" or the "NOT" gate. (b) The detailed mechanism of the all-optical logic operations. The black and red numbers are the input binary logic values and the output levels, respectively. Terminals labeled with "Control" indicate that the control port is turned on, which can provide power for the operation of the "NOT" gate.

the geometric dimensions of the meta-atom. Rotation matrix $R(\theta) = \begin{pmatrix} \cos\theta & \sin\theta \\ -\sin\theta & \cos\theta \end{pmatrix}$ is a real unitary matrix with a rotation angle θ relative to the reference coordinate axis[11]. Then, the Jones matrix can be formulated as a symmetric and unitary matrix,

$$J = \begin{pmatrix} \cos^2\theta e^{i\phi_x} + \sin^2\theta e^{i\phi_y} & \sin\theta\cos\theta(e^{i\phi_x} - e^{i\phi_y}) \\ \sin\theta\cos\theta(e^{i\phi_x} - e^{i\phi_y}) & \cos^2\theta e^{i\phi_y} + \sin^2\theta e^{i\phi_x} \end{pmatrix} = \begin{pmatrix} e^{i\phi_1} & e^{i\phi_2} \\ e^{i\phi_2} & e^{i\phi_3} \end{pmatrix}. \quad (2)$$

Due to the symmetry of the metasurface, it owns three independent degrees of freedom, i.e., phases ϕ_1, ϕ_2, and ϕ_3, which can be individually controlled by the cooperation of the propagation phase and geometric phase[23,28,29]. Under the incidence of the circularly polarized lights $(1 \quad \pm i)^T$, the transmitted light field can be expressed as

$$E_{\text{out}}^{\text{RCP/LCP}} = J \cdot E_{\text{in}}^{\text{RCP/LCP}} = \begin{pmatrix} e^{i\phi_1} + e^{i(\phi_2 \pm \frac{\pi}{2})} \\ e^{i\phi_2} + e^{i(\phi_3 \pm \frac{\pi}{2})} \end{pmatrix} = e^{i\phi_1}\begin{pmatrix} 1 \\ 0 \end{pmatrix} + e^{i(\phi_3 \pm \frac{\pi}{2})}\begin{pmatrix} 0 \\ 1 \end{pmatrix} + e^{i(\phi_2 \pm \frac{\pi}{2})}\begin{pmatrix} 1 \\ \mp i \end{pmatrix}, \quad (3)$$

where "+" and "−" are, respectively, denoted as RCP and LCP. The output field comprises three different polarized components, i.e., the X linearly polarized light with a phase profile of ϕ_1, the Y linearly polarized light with a phase profile of ϕ_3, and the circularly polarized light with a phase profile of ϕ_2.

Note that LCP and RCP can be added to form a linearly polarized light vibrating in the X direction. Illuminated by the XLP light with a Jones vector of $(1 \quad 0)^T$, the output field of the metalens can be expressed as

$$E_{\text{out}}^{\text{XLP}} = J \cdot E_{\text{in}}^{\text{XLP}} = \begin{pmatrix} e^{i\phi_1} \\ e^{i\phi_2} \end{pmatrix} = e^{i\phi_1}\begin{pmatrix} 1 \\ 0 \end{pmatrix} + e^{i\phi_2}\begin{pmatrix} 0 \\ 1 \end{pmatrix}. \quad (4)$$

The output field comprises two different polarized components, namely, the X linearly polarized light with a phase profile of ϕ_1 and the Y linearly polarized light with a phase profile of ϕ_2.

As formulated by Eqs. (3) and (4), one can extract phases ϕ_1, ϕ_2, and ϕ_3 from the output results under the input of only the RCP or LCP, and ϕ_1 and ϕ_2 can be extracted when two channels are activated at the same time. To realize the above-mentioned parallel logic operations, the encoded ϕ_1 is used for the construction of the "OR" gate, and ϕ_3 is designed for the construction of the "XOR" or the "NOT" gate. Noticeably, the additional phase ϕ_2 is assigned to a random phase profile with negligible crosstalk to the logic operations.

To display the binary logic intuitively, off-axis focusing is implemented using the required phase ϕ_i $(i = 1, 3)$, which can be expressed as

$$\phi_i = \frac{w}{c}\left[f - \sqrt{(x - d_x^i)^2 + (y - d_y^i)^2 + f^2}\right] + \phi_c^i, \quad (5)$$

where (d_x^i, d_y^i) is the local position of the focus on the focal plane; and f, w, and c, respectively, represent the focal length, optical

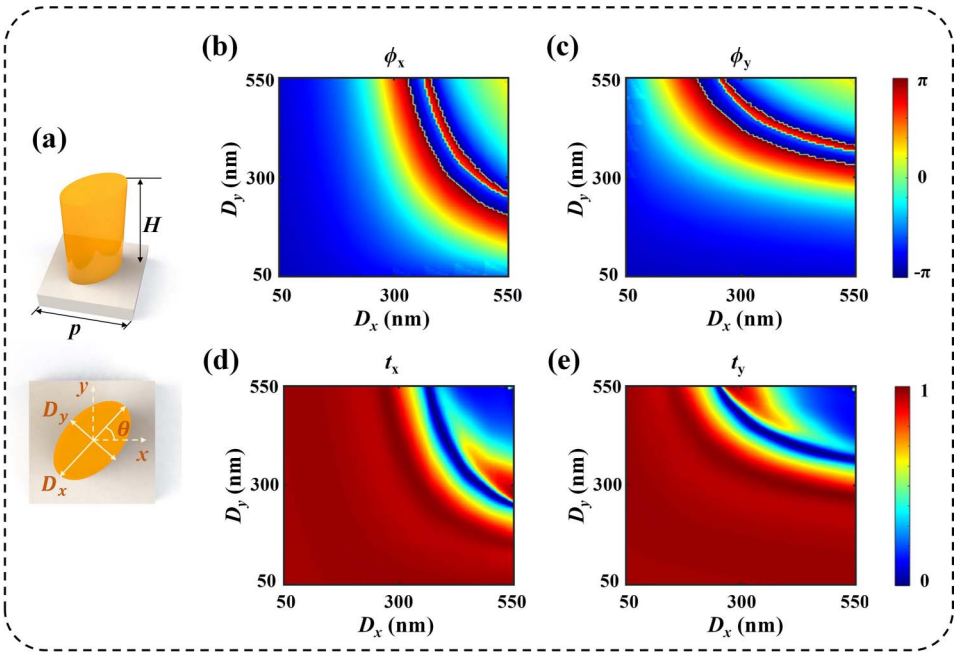

Fig. 2. Design of the meta-atom library. (a) Schematic illustration of a single Si nanopillar placed on a rectangular SiO_2 substrate. (b)–(e) The optical responses of the meta-atom at the wavelength of 1550 nm. Phase shifts ϕ_x (b) and transmittance t_x (d) under the XLP incidence. Phase shifts ϕ_y (c) and transmittance t_y (e) under the YLP incidence.

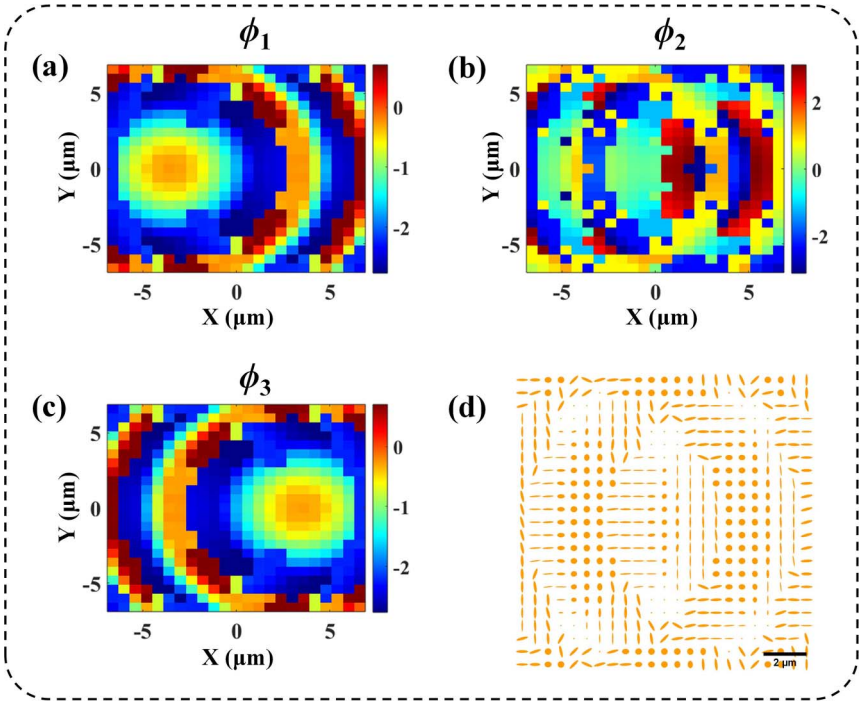

Fig. 3. Design of the metasurface-based logic operator. (a) Phase ϕ_1 is used for the construction of the "OR" gate. (b) Phase ϕ_2 is assigned to a random phase profile with negligible crosstalk to the logic operations. (c) Phase ϕ_3 used for the construction of "XOR" or "NOT" gate. (d) Top view of the metasurface.

angular frequency, and speed of light in vacuum. ϕ_c^i is a constant reference phase, which can be used to optimize the design of the proposed metalens.

To achieve the proposed Jones matrix metalens, the meta-atom library is constructed, as shown in Fig. 2. The meta-atom is a simple silicon (Si) elliptical nanopillar and periodically located on a rectangular silicon dioxide (SiO_2) substrate with a fixed height of $H = 1200$ nm and a period of $P = 600$ nm. The propagation phase can be manipulated by shaping the elliptical major axis (D_x) and the minor axis (D_y) of the nanopillars. Thus, the functional relationship between (ϕ_x, ϕ_y) and (D_x, D_y) can be established without altering the orientation angle (θ). The elliptical major axis and minor axis of the nanopillar are both swept from 50 nm to 550 nm, and the phase shifts ϕ_x under the XLP incidence at an incident wavelength of 1550 nm are shown in Fig. 2(b). Due to the symmetry, phase shifts ϕ_y under the YLP incidence are the transposition of phase shifts ϕ_x, as shown in Fig. 2(c). They both realize the full coverage of the 0 to 2π range to ensure all phases available. Moreover, the influence of distinct amplitudes should be minimized to ensure the high efficiency of the optical signal processing. Figures 2(d) and 2(e) depict the transmittances of the designed meta-atoms. Most of the transmittances are nearly joined. The geometric phase also needs to be considered in our design, which is adjusted by altering the orientation angle (θ). Then, the flexible control of the Jones matrix can be implemented by building the functional relationship between (ϕ_x, ϕ_y, and θ) and (ϕ_1, ϕ_2, and ϕ_3).

Figure 3 illustrates the phase profiles of the metasurface and the arrangements of the meta-atoms at corresponding positions. In this work, three phases (ϕ_1, ϕ_2, ϕ_3) are simultaneously encoded into three independent channels of the Jones matrix polarization-switchable metasurface. Phase ϕ_1 is used for the construction of the "OR" gate, ϕ_3 is used for the "XOR" or the "NOT" gate, and ϕ_2 is assigned to a random phase profile with negligible crosstalk to the logic operations. Thus, the two spatially separated focus spots can be flexibly manipulated with varied polarization inputs, which can perform corresponding optical logic operations.

3. Results

To further verify the above theoretical analysis, a polarization-multiplexed metalens is designed with a focal length of 17 μm, a dimension of 14 μm × 14 μm, and off-axis parameters of $d_x^1 = -3.5$ μm, $d_x^3 = 3.5$ μm, and $d_y^i = 0$ μm. As shown in Fig. 4, simulation results of the intensity profiles on the axial plane (X–Z cross section) are extracted reasonably under the RCP, the LCP, and the XLP incidence, which is consistent with the results of the theoretical derivation. For the RCP or LCP incidence [explained by Eq. (3)], the output X component is a tilted focal spot along the negative x-axis [Figs. 4(a) and 4(d)], which is dominated by phase ϕ_1 with a focus located at $x = -3.5$ μm and $z = 17$ μm. The output Y component depicts a tilted focal spot along the positive x axis [Figs. 4(b) and 4(e)], which is controlled by ϕ_3 with a focus located at $x = 3.5$ μm and $z = 17$ μm. The total output field shows two tilted focal spots along the negative and positive x-axis, respectively [Figs. 4(c) and 4(f)], which is the

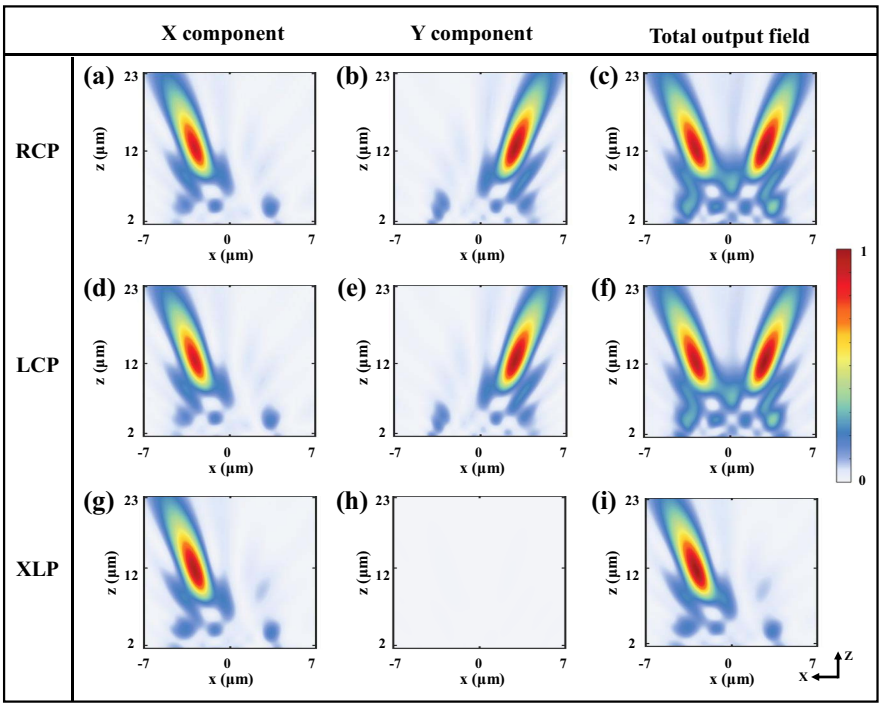

Fig. 4. Simulation results of the extracted intensity profiles under diverse polarized light. (a)–(c) Output *X* component, *Y* component, and the total output field with RCP incidence. (d)–(f) Output *X* component, *Y* component, and the total output field with LCP incidence. (g)–(i) Output *X* component, *Y* component, and the total output field with XLP incidence.

common work of ϕ_1, ϕ_2, and ϕ_3. The output fields are almost unaffected by the background noise mainly caused by random phase ϕ_2. For the XLP incidence [explained by Eq. (4)], the output X component is a tilted focal spot along the negative x-axis [Fig. 4(g)], which is dominated by the off-axis focusing phase profile ϕ_1, and the output Y component shows no clear

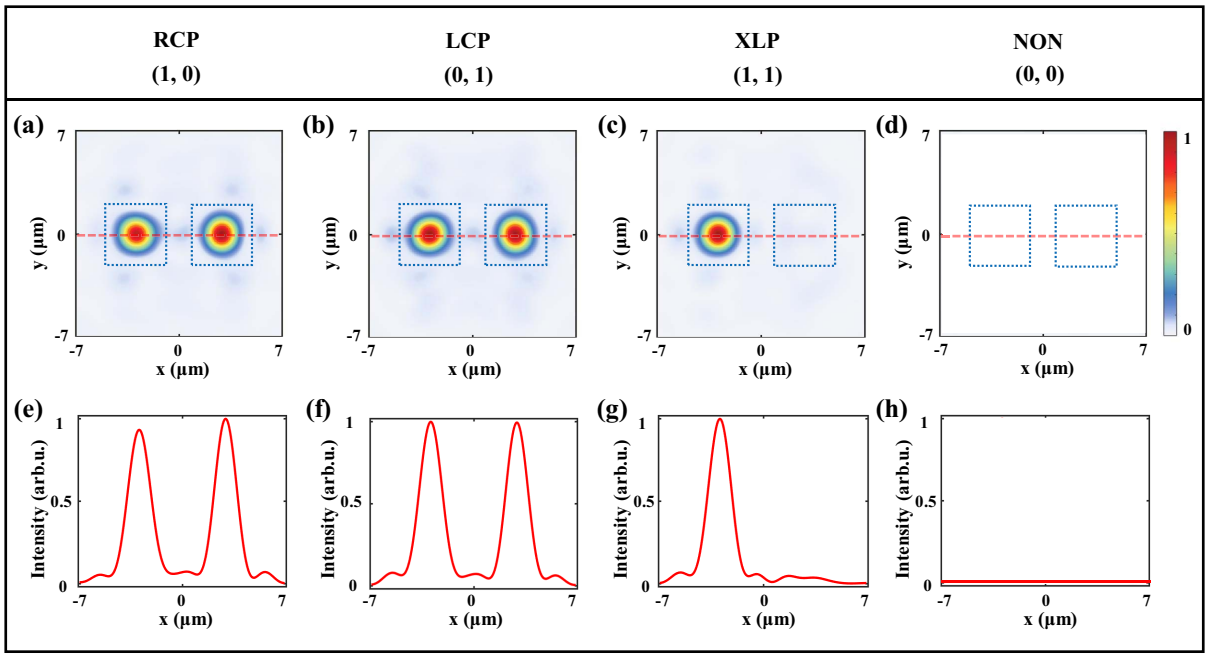

Fig. 5. Numerical demonstration of the proposed parallel logic processor. (a)–(d) Output normalized intensity distribution, with each corresponding to one exact input logic state. On each focal plane, the left highlighted region is used as the "OR" gate, and the right is designed for the "XOR" or the "NOT" gate. (e)–(h) Normalized intensity distribution along the *x*-axis of (a)–(d).

focal spot [Fig. 4(h)], which is determined by the random phase profile ϕ_2. Since the total output field is the common work of ϕ_1 and ϕ_2, the total output field shows a tilted focal spot along the negative x-axis [Fig. 4(i)]. The extracted intensity profiles under diverse polarized light show that this method is suitable for all-optical logic operations based on metasurface polarization optics.

Figure 5 shows the numerical demonstration of the parallel logic processor. As shown in Figs. 5(a)–5(d), the results of the parallel logic operations are displayed in the highlighted dashed squares of each focal plane, where the left one is used for the "OR" gate and the right is for the "XOR" or the "NOT" gate. Here, the output logic levels "1" and "0" are distinguished by the power concentrated in the focus spot and by the faint speckles, and the high optical power contrast can ensure the effectiveness and functionality of the proposed logic gates. The output phenomenon is obvious and clear, which is consistent with the theoretical derivation of the proposed parallel logic processor. In addition, phase superposition coding of the two logic gates will result in channel expansion with almost negligible crosstalk. Figures 5(e)–5(h) indicate that the light intensity is well confined within the designed logic operation region. The two foci are located at $x = -3.4\,\mu m$, $y = 0\,\mu m$ and $x = 3.4\,\mu m$, $y = 0\,\mu m$, respectively. Both are consistent with the design of the off-axis parameters. The focusing efficiency is defined as the ratio of the energy in three times of the full-width at half-maximum region to the energy of the incident light[23]. The focusing efficiencies of the two designed areas are 40.7% and 41.1% at 1550 nm. The slight deviations from the theoretical values are due to the relatively small size of the proposed metalens and phase errors. Here, the output binary logic state can be measured as long as two probes are placed at the center of the two focal spots. This means that post-processing can be streamlined and implemented by using point detections.

4. Conclusion

In summary, we have demonstrated a unique scheme for parallel dual logic processing based on metasurface polarization optics. The "OR" gate, the "XOR" gate, or the "NOT" gate can be realized by a single-layer metasurface, which makes a step towards higher integration density and compactness and its own capability of the accessible multifunctionalities, since the logic processor is assigned by flexible and adjustable wavefront engineering. Thus, the parallel logic operator can result in the expansion of a few working channels without reducing the quality of signal processing, which facilitates the ability to process information synchronously. In addition, this strategy has the potential to operate over a broad waveband as chromatic aberration can be eliminated by the method of chromatic engineering. Parallel processing and compactness are the unique advantages of the metasurface-based logic processors, which may find applications in the fields of computing and communication integrated in all-optical or hybrid optical-electronic systems.

Acknowledgement

This work was supported by the National Key Research and Development Program of China (No. 2019YFE0107400) and the National Natural Science Foundation of China (No. 52005147).

References

1. D. R. Solli and B. Jalali, "Analog optical computing," Nat. Photonics **9**, 704 (2015).
2. R. Athale and D. Psaltis, "Optical computing: past and future," Opt. Photonics News **27**, 32 (2016).
3. C. Wu, H. Yu, S. Lee, R. Peng, I. Takeuchi, and M. Li, "Programmable phase-change metasurfaces on waveguides for multimode photonic convolutional neural network," Nat. Commun. **12**, 96 (2021).
4. H. J. Caulfield and S. Dolev, "Why future supercomputing requires optics," Nat. Photonics **4**, 261 (2010).
5. W. Ying, X. Fan, J. Gu, S. Xu, and S. Liu, "Oxyfluoride glass-ceramics for upconversion all-optical combinational logic gate operations," Cell Rep. Phys. Sci. **3**, 100871 (2022).
6. H. Wei, Z. Wang, X. Tian, M. Käll, and H. Xu, "Cascaded logic gates in nanophotonic plasmon networks," Nat. Commun. **2**, 387 (2011).
7. Y. Sang, X. Wu, S. S. Raja, C.-Y. Wang, H. Li, Y. Ding, D. Liu, J. Zhou, H. Ahn, S. Gwo, and J. Shi, "Broadband multifunctional plasmonic logic gates," Adv. Opt. Mater. **6**, 1701368 (2018).
8. M. W. McCutcheon, G. W. Rieger, J. F. Young, D. Dalacu, P. J. Poole, and R. L. Williams, "All-optical conditional logic with a nonlinear photonic crystal nanocavity," Appl. Phys. Lett. **95**, 221102 (2009).
9. K. Li, H.-F. Ting, M. A. Foster, and A. C. Foster, "High-speed all-optical NAND/AND logic gates using four-wave mixing Bragg scattering," Opt. Lett. **41**, 3320 (2016).
10. N. Yu, P. Genevet, M. A. Kats, F. Aieta, J.-P. Tetienne, F. Capasso, and Z. Gaburro, "Light propagation with phase discontinuities: generalized laws of reflection and refraction," Science **334**, 333 (2011).
11. J. P. Balthasar Mueller, N. A. Rubin, R. C. Devlin, B. Groever, and F. Capasso, "Metasurface polarization optics: independent phase control of arbitrary orthogonal states of polarization," Phys. Rev. Lett. **118**, 113901 (2017).
12. S. Zahra, L. Ma, W. Wang, J. Li, D. Chen, Y. Liu, Y. Zhou, N. Li, Y. Huang, and G. Wen, "Electromagnetic metasurfaces and reconfigurable metasurfaces: a review," Front. Phys. **8**, 593411 (2021).
13. S. Wang, P. C. Wu, V.-C. Su, Y.-C. Lai, M.-K. Chen, H. Y. Kuo, B. H. Chen, Y. H. Chen, T.-T. Huang, J.-H. Wang, R.-M. Lin, C.-H. Kuan, T. Li, Z. Wang, S. Zhu, and D. P. Tsai, "A broadband achromatic metalens in the visible," Nat. Nanotechnol. **13**, 227 (2018).
14. W. T. Chen, A. Y. Zhu, V. Sanjeev, M. Khorasaninejad, Z. Shi, E. Lee, and F. Capasso, "A broadband achromatic metalens for focusing and imaging in the visible," Nat. Nanotechnol. **13**, 220 (2018).
15. J. Park, B. G. Jeong, S. I. Kim, D. Lee, J. Kim, C. Shin, C. B. Lee, T. Otsuka, J. Kyoung, S. Kim, K.-Y. Yang, Y.-Y. Park, J. Lee, I. Hwang, J. Jang, S. H. Song, M. L. Brongersma, K. Ha, S.-W. Hwang, H. Choo, and B. L. Choi, "All-solid-state spatial light modulator with independent phase and amplitude control for three-dimensional LiDAR applications," Nat. Nanotechnol. **16**, 69 (2021).
16. G. E. Lio and A. Ferraro, "LIDAR and beam steering tailored by neuromorphic metasurfaces dipped in a tunable surrounding medium," Photonics **8**, 65 (2021).
17. J. Li, Y. Chen, Y. Hu, H. Duan, and N. Liu, "Magnesium-based metasurfaces for dual-function switching between dynamic holography and dynamic color display," ACS Nano **14**, 7892 (2020).
18. J. Kim, Y. Yang, T. Badloe, I. Kim, G. Yoon, and J. Rho, "Geometric and physical configurations of meta-atoms for advanced metasurface holography," InfoMat **3**, 739 (2021).
19. Z. Zhao, Y. Wang, C. Guan, K. Zhang, Q. Wu, H. Li, J. Liu, S. N. Burokur, and X. Ding, "Deep learning-enabled compact optical trigonometric operator with metasurface," PhotoniX **3**, 15 (2022).

20. X. Zhang, L. Huang, R. Zhao, H. Zhou, X. Li, G. Geng, J. Li, X. Li, Y. Wang, and S. Zhang, "Basis function approach for diffractive pattern generation with Dammann vortex metasurfaces," Sci. Adv. **8**, eabp8073 (2022).
21. C. Qian, X. Lin, X. Lin, J. Xu, Y. Sun, E. Li, B. Zhang, and H. Chen, "Performing optical logic operations by a diffractive neural network," Light Sci. Appl. **9**, 59 (2020).
22. Z. Zhao, Y. Wang, X. Ding, H. Li, J. Fu, K. Zhang, S. N. Burokur, and Q. Wu, "Compact logic operator utilizing single-layer metasurface," Photonics Res. **10**, 316 (2021).
23. L. Li, J. Zhang, Y. Hu, J. Lai, S. Wang, P. Yang, X. Li, and H. Duan, "Broadband polarization-switchable multi-focal noninterleaved metalenses in the visible," Laser Photonics Rev. **15**, 2100198 (2021).
24. D. Zhong, Y. Ji, and W. Luo, "Controllable optoelectric composite logic gates based on the polarization switching in an optically injected VCSEL," Opt. Express **23**, 29823 (2015).
25. D. Zhong, G. Yang, Z. Xiao, Y. Ding, J. Xi, N. Zeng, and H. Yang, "Optical chaotic data-selection logic operation with the fast response for picosecond magnitude," Opt. Express **27**, 23357 (2019).
26. D. Zhong, Z. Xiao, G. Yang, N. Zhen, and H. Yang, "Real-time ranging of the six orientational targets by using chaotic polarization radars in the three-node VCSEL network," Opt. Express **27**, 9857 (2019).
27. D.-Z. Zhong, G.-L. Xu, W. Luo, and Z.-Z. Xiao, "Reconfigurable dynamic all-optical chaotic logic operations in an optically injected VCSEL," Chin. Phys. B **26**, 124204 (2017).
28. R. Zhao, B. Sain, Q. Wei, C. Tang, X. Li, T. Weiss, L. Huang, Y. Wang, and T. Zentgraf, "Multichannel vectorial holographic display and encryption," Light Sci. Appl. **7**, 95 (2018).
29. Y. Hu, L. Li, Y. Wang, M. Meng, L. Jin, X. Luo, Y. Chen, X. Li, S. Xiao, H. Wang, Y. Luo, C.-W. Qiu, and H. Duan, "Trichromatic and tripolarization-channel holography with noninterleaved dielectric metasurface," Nano Lett. **20**, 994 (2019).